A Joint-Limits Avoidance Strategy for Arc-Welding Robots

Luc Baron
Département de génie mécanique
École Polytechnique, C.P. 6079, succ. CV
Montréal, Québec, Canada H3C 3A7
E-mail: baron@meca.polymtl.ca

Résumé: En raison de la symétrie de l'électrode de soudage autour de son axe, les opérations de soudage peuvent être réalisées avec seulement cinq degrés-de-liberté (DDL). Néanmoins, lorsque réalisées par des robots à six DDL, une stratégie d'évitement des limites articulaires peut être implantée en utilisant une matrice Jacobienne augmentée, ainsi qu'un vecteur de vitesses articulaires augmentées, par une rotation virtuelle autour de l'axe de l'électrode. Dans cet article, nous étudions l'efficacité et l'adéquation de cette approche.

Abstract: Because of the symmetry of the welding tool around the electrode axis, arc-welding operations can be realized with only five degrees-of-freedom (DOF). However, when performed with six-DOF robots, a joint-limits avoidance strategy can be implemented on an augmented Jacobian matrix, and its corresponding augmented joint-rate vector, by a virtual rotation around the electrode axis. This approach has proven to be efficient and effective.

Introduction: With an arc-welding robot, the programming of a tool path is usually performed in two steps. First, the welding cord is discretized into a set of 3D poses—i.e. position and orientation—, each being described by the position vector $\mathbf{p}$ of the tool-tip with respect to the origin of the part frame $\mathcal{P}$ and the unit vector, namely $\mathbf{q}$, along the tool axis and pointing toward the tool-holding end, both expressed in frame $\mathcal{P}$. Second, this set of 3D poses is mapped from *Cartesian space* to *joint space* with the inverse kinematic model of the welding robot.

This trajectory planning problem can be resolved through the computation of the *Darboux* vector of the path and its time derivative, which also prescribes the angular velocity and acceleration of the welding tool with respect to $\mathcal{P}$. As shown in [1], this approach requires to compute the unit tangent, normal and binormal vectors of a given tool-path, and then solve the inverse kinematic problem for each of the computed triad. Although the tool path being continuous in Cartesian space with this approach, its corresponding path in joint space may not be continuous.

Moreover, it is noted that the orientation of the tool around the electrode axis is irrelevant to the welding operation, and hence, this task can be performed with only a five-degrees-of-freedom (DOF). However, if the task is realized with a six-DOF robot, there is one DOF of redundancy, and it is possible to implement a secondary control strategy, like the avoidance of joint limits.

Problem Formulation: This subject of redundancy-resolution has already been studied at both joint-position level [2, 3] and at joint-rate level [4, 5]. Here, we

adopt the joint-rate formulation because the redundancy-resolution problem is linear at that level. The Jacobian of a six-DOF welding robot, namely $\mathbf{J}$, maps the joints-rate $\dot{\boldsymbol{\theta}}$ into the twist $\mathbf{t}$ of the welding tool as follows:

$$\mathbf{J}\dot{\boldsymbol{\theta}} = \mathbf{t}, \tag{1}$$

where $\dot{\boldsymbol{\theta}}$ and $\mathbf{t}$ are defined as

$$\dot{\boldsymbol{\theta}} \equiv [\dot{\theta}_1 \cdots \dot{\theta}_6]^T, \mathbf{t} \equiv [\boldsymbol{\omega}^T \dot{\mathbf{p}}]^T, \tag{2}$$

with $\boldsymbol{\omega}$ and $\dot{\mathbf{p}}$ being the angular and translational velocities of the welding tool with respect to the origin of $\mathcal{P}$ and expressed in $\mathcal{P}$. There are two different approaches to account for five-DOF tasks using a six-DOF twist. First, one can project the first three lines of $\mathbf{J}$ and the first part of $\mathbf{t}$, i.e. $\boldsymbol{\omega}$, onto the plan perpendicular to the electrode axis. With this approach, the inverse kinematic problem reduces to the determination of the joint-rates of a projected Jacobian onto a projected twist. However, projectors are always *singular*, and hence, the particular structure of the projection of $\boldsymbol{\omega}$ needs to be taken into account when solving for the projected Jacobian. The second approach assumes a virtual rotation, namely θ_w, of the tool-tip around the electrode axis. Although this rotation does not exist, it is added to the Jacobian and the joint-rate in order to obtain an underdetermined linear algebraic system with at least one-DOF of redundancy. This second approach is preferred since it is much straightforward then the first.

The Jacobian of the robot augmented by the virtual joint-rate $\dot{\theta}_w$ around the welding tool axis, namely $\mathbf{J}_w$, maps the augmented joints-rate $\dot{\boldsymbol{\theta}}_w$ into the twist $\mathbf{t}$ of the welding tool as

$$\mathbf{J}_w\dot{\boldsymbol{\theta}}_w = \mathbf{t}, \tag{3}$$

where $\dot{\boldsymbol{\theta}}_w$ is defined as

$$\dot{\boldsymbol{\theta}}_w \equiv [\dot{\boldsymbol{\theta}}^T \dot{\theta}_w]^T. \tag{4}$$

Joint-Limits Avoidance Strategy: The solution of eq.(3) is well-known to be

$$\dot{\boldsymbol{\theta}}_w = \mathbf{J}_w^{\dagger}\mathbf{t} + (\mathbf{1} - \mathbf{J}_w^{\dagger}\mathbf{J}_w)\mathbf{h}, \tag{5}$$

with $\mathbf{h}$ being a secondary task and $\mathbf{J}_w^{\dagger}$ the right generalized inverse of $\mathbf{J}_w$, i.e., $\mathbf{J}_w^{\dagger} = \mathbf{J}_w^T(\mathbf{J}_w\mathbf{J}_w^T)^{-1}$. Moreover, $(\mathbf{1} - \mathbf{J}_w^{\dagger}\mathbf{J}_w)$ is an orthogonal complement of $\mathbf{J}_w$ projecting $\mathbf{h}$ onto the nullspace of $\mathbf{J}_w$. Thus, $(\mathbf{1} - \mathbf{J}_w^{\dagger}\mathbf{J}_w)\mathbf{h}$ is an homogeneous solution of eq.(3), which corresponds to the self-motion of $\mathbf{J}_w$, i.e., a motion of $\dot{\boldsymbol{\theta}}$ and $\dot{\theta}_w$ under which the tool tip remains stationary relative to the part. Since $\dot{\theta}_w$ is only virtual, the self-motion of $\mathbf{J}_w$ is equivalent to the motion of $\dot{\boldsymbol{\theta}}$ under which the tool-tip position and only the tool-axis orientation remain stationary relative to the part.

The secondary task is chosen as $\mathbf{h} = \nabla z$, where z is defined as the following objective function, namely,

$$z = \frac{1}{2}(\boldsymbol{\theta} - \bar{\boldsymbol{\theta}})^T\mathbf{W}(\boldsymbol{\theta} - \bar{\boldsymbol{\theta}}), \tag{6}$$

where $\mathbf{W}$ is a positive-definite weighting matrix and $\bar{\boldsymbol{\theta}}$ is computed as either the mid-joint robot position computed as

$$\boldsymbol{\theta}_R \equiv \frac{1}{2}(\boldsymbol{\theta}_{max} + \boldsymbol{\theta}_{min}), \tag{7}$$

or the mean-joint robot position along the welding tool path Λ, i.e.,

$$\boldsymbol{\theta}_\Lambda \equiv \frac{\oint_\Lambda \boldsymbol{\theta}(t)dt}{\oint_\Lambda dt}, \tag{8}$$

where t is the time. Clearly, this optimization problem allows the tool tip and axis to remain along the welding tool-path, while keeping the position of the joint axes of the robot at the closest distance from either the mid-joint or mean-joint robot position. The weighting matrix $\mathbf{W}$ is chosen as a diagonal matrix whose elements are determined by allowable deviations from this mid- or mean-joint position.

Numerical Implementation: In this paper, we use the orthogonalization scheme proposed by Arenson et al. [6] in order to render $\mathbf{J}_w$ into lower-triangular form, while preserving its condition number. In this approach, the redundancy-resolution is computed without requiring a direct calculation of the generalized inverse of $\mathbf{J}_w$, and hence, avoid the squaring of the condition number of the problem. We recall that the condition number of a problem expresses the lost of accuracy during its solution. For the control of welding operations, the squaring of the errors is obviously unacceptable.

Pipe-Bride Welding Application: The strategy has been implemented within a simulation module and tested with the architecture of the Puma 560 manipulator together with a generic arc-welding tool such as describes with the Denavit-Hartenbrg parameters of Table 1. For quick reference, we shortly recall the meaning of these parameters below. Let us attach frame $\mathcal{F}_i$ to link i with the z_i-axis aligned with the axis of joint $i+1$, and the x_i-axis aligned along the common perpendicular to the axes of joints i and $i+1$. The first parameter θ_i is the joint rotation around z_i-axis; b_i is the translation distance along z_i-axis of the origin of $\mathcal{F}_i$ up to the common perpendicular with $\mathcal{F}_{i+1}$; a_i is the length of this common perpendicular; while α_i is the rotation around the common perpendicular toward $\mathcal{F}_{i+1}$.

Table 1: Denavit-Hartenberg parameters of the Puma 560 with a generic welding tool

joint	θ_i	a_i	b_i	α_i
1	θ_1	0.0	0.0	-$\pi/2$
2	θ_2	0.4318	0.0	0.0
3	θ_3	-0.0203	0.1491	$\pi/2$
4	θ_4	0.0	0.4330	-$\pi/2$
5	θ_5	0.0	0.0	$\pi/2$
6	θ_6	0.0	0.7294	$\pi/6$
7	θ_7	0.0	-0.2000	0.0
unit	rad.	m	m	rad.

It is noteworthy that Table 1 includes a virtual seventh joint, namely θ_7, which obviously does not exist, and thus, is not controlled by the robot. The purpose of this seventh joint is to describe the gain of freedom of the task due to the use of a symmetric electrode. The control of this virtual 7-DOF robot along a fully constrained 6-DOF task with $\mathbf{t} = \mathbf{J}_w \boldsymbol{\theta}_w$ is equivalent to the control of the original 6-DOF robot along the 5-DOF welding task with $\mathbf{t} = \mathbf{J}_{\boldsymbol{\theta}}$. In both cases, the robot has one-DOF more than the task, and hence, there is one-DOF of redundancy to resolve with the joint-limits avoidance strategy.

The robot is aimed to perform a pipe-bride welding trajectory Λ in $T = 280 sec.$, i.e.,

$$\mathbf{p} = \begin{bmatrix} 0.1\cos(\omega t) \\ 0.6 + 0.1\sin(\omega t) \\ -0.59 \end{bmatrix}, \qquad (9)$$

$$\mathbf{R} = \begin{bmatrix} \cos\alpha & -\sin\alpha\cos\beta & \sin\alpha\sin\beta \\ \sin\alpha & \cos\alpha\cos\beta & \cos\alpha\cos\beta \\ 0 & \sin\beta & \cos\beta \end{bmatrix},$$

with

$$\alpha = \tfrac{\pi}{2} + \omega t, \quad \beta = \tfrac{-3\pi}{4}, \quad \omega = \tfrac{2\pi}{T}, \quad 0 \le t \le T, \qquad (10)$$

where distances and angles are, respectively, expressed in meter and radian.

Figure 1 shows the time history of the joint positions of the robot along the given welding trajectory without taking into account the symmetry of the welding electrode. The corresponding time history of the robot task is illustrated in fig.4. Apparently, the robot is able to perform the task while using the full amplitude of its joint motion. A second consecutive turn is, obviously, not possible without exceeding the joint limits.

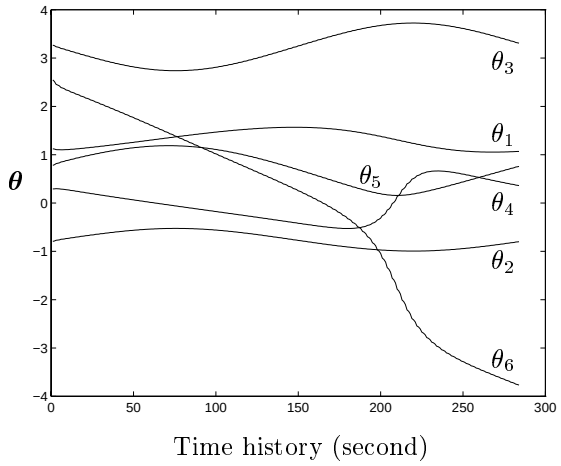

Figure 1: Joint positions without joint-limits avoidance strategy

Figure 2 shows the time history of the joint positions of the robot along the same trajectory, but the control is performed with the augmented Jacobian and joint-rate vector together with the mid-joint robot strategy, with $\boldsymbol{\theta}_R = [0,\ -\pi/2,\ \pi/2,\ 0,\ 0,\ 0]^T$. The corresponding time history of the robot task is illustrated in fig.5. Apparently, the robot is able to perform the task while using much less amplitude of its joint motion. Here again, a second consecutive turn is not possible without exceeding the joint limits.

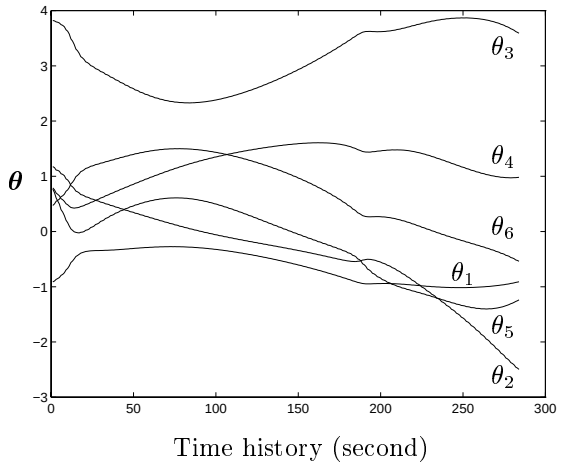

Figure 2: Joint positions with the mid-joint avoidance strategy

Figure 3 shows the time history of the joint positions of the robot along the same trajectory, the control is here performed with the augmented Jacobian and joint-rate vector together with the mean-joint robot strategy, with $\boldsymbol{\theta}_\Lambda = [\pi/2,\ -\pi/3,\ \pi,\ 0,\ \pi/3,\ 0]^T$. The corresponding time history of the robot task is illustrated in fig.6. Apparently, the robot is still able to perform the task while using approximately the same amplitude of its joint motion. Moreover, multiple consecutive turns are here possible without exceeding the joint limits, and hence, a cycloidal trajectory is possible with this strategy. In fact, the robot starts and ends the circular trajectory with exactly the same joint positions.

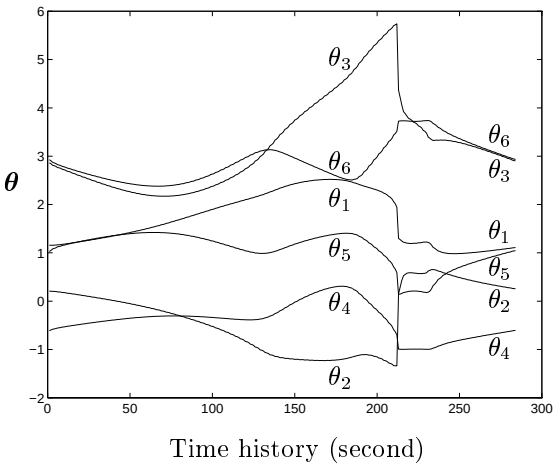

Figure 3: Joint positions with the mean-joint avoidance strategy

Clearly, the resulting trajectory in joint space with the mid-joint avoidance strategy (i.e., $\bar{\boldsymbol{\theta}} = \boldsymbol{\theta}_R$) depends on the relative position and orientation of the assembly with respect to the mid-joint position. A displacement of the assembly dramatically changes the cycloidal or non-cycloidal nature of the resulting trajectory in joint space. Conversely, the mean-joint avoidance strategy (i.e., $\bar{\boldsymbol{\theta}} = \boldsymbol{\theta}_\Lambda$) allows to keep the cycloidal nature of the trajectory in joint space trajectory. However, a displacement of the assembly within the

robot workspace does not guaranty the capacity of the robot to perform the trajectory in joint space without exceeding the joint limits. In fact, a selection of the position and orientation of the assembly leads to a mean-joint position, which must be as close as possible to the mid-joint position, in order to reduce to a minimum the probability of exceeding the joint limits. Thus, the optimal positions and orientations of the assembly are those that are solutions of the following equation, i.e.,

$$\boldsymbol{\theta}_R = \frac{\oint_\Lambda \boldsymbol{\theta}(t)dt}{\oint_\Lambda dt} \tag{11}$$

for a given trajectory Λ free to translate and rotate, along and around, any axis.

Conclusions: A joint-limits avoidance strategy has been presented for arc-welding operations, where the task gain one-DOF due to the symmetry of the electrode relatively to its axis. In this situation, the welding task can be realized with only five-DOF robots. However, when realized with six-DOF robots, it is possible to implement a joint limits avoidance strategy on an augmented Jacobian matrix and an augmented joint-rate vector by a virtual seventh rotation around the electrode axis. With this augmented approach, it is possible to find cycloidal trajectories in joint space that avoid the joint limits under a proper location of the assembly within the robot workspace.

Acknowledgement: The financial support from the Natural Sciences and Engineering Research Council of Canada under grant OGPIN-203618 is gratefully acknowledged.

References

[1] Angeles, J., Roja, A. and López-Cajú, C. S., 1988, "Trajectory Planning in Robotics Continous-Path Applications", *IEEE Journal of Robotics and Automation*, Vol. 4, No. 4, pp. 380–385.

[2] Yashi, O.S. and Ozgoren, K., 1984, "Minimal Joint Motion Optimization of Manipulators with Extra degrees of freedom", *Mechanism and Machine Theory*, Vol. 19, No. 3, pp. 325–330.

[3] Angeles, J., Anderson, K. and Gosselin, C., 1987, "An Orthogonal-Decomposition Algorithm for Constrained Least-Square Optimization", *ASME Robotics, Mechanisms, and Machine Systems, Design Eng. Division*, Vol. 2, pp. 215–220.

[4] Ballieul, J., 1985, "Kinematic Programming Alternatives for Redundant Manipulators", *IEEE Int. Conference on Robotics and Automation*, pp. 723–730.

[5] Siciliano, B., 1992, "Solving Manipulator Redundancy with the Augmented Task Space Method Using the Constraint Jacobian Transpose", *IEEE Int. Conference on Robotics and Automation*, Tutorial M1, pp. 5-1–5-8.

[6] Arenson, N., Angeles, J. and Slutski, L., 1998, "Redundancy-Resolution Algorithms for Isotropic Robots", *Advances in Robot Kinematics: Analysis and Control*, Kluwer Academic Publishers, Dordrecht, pp. 425–434.

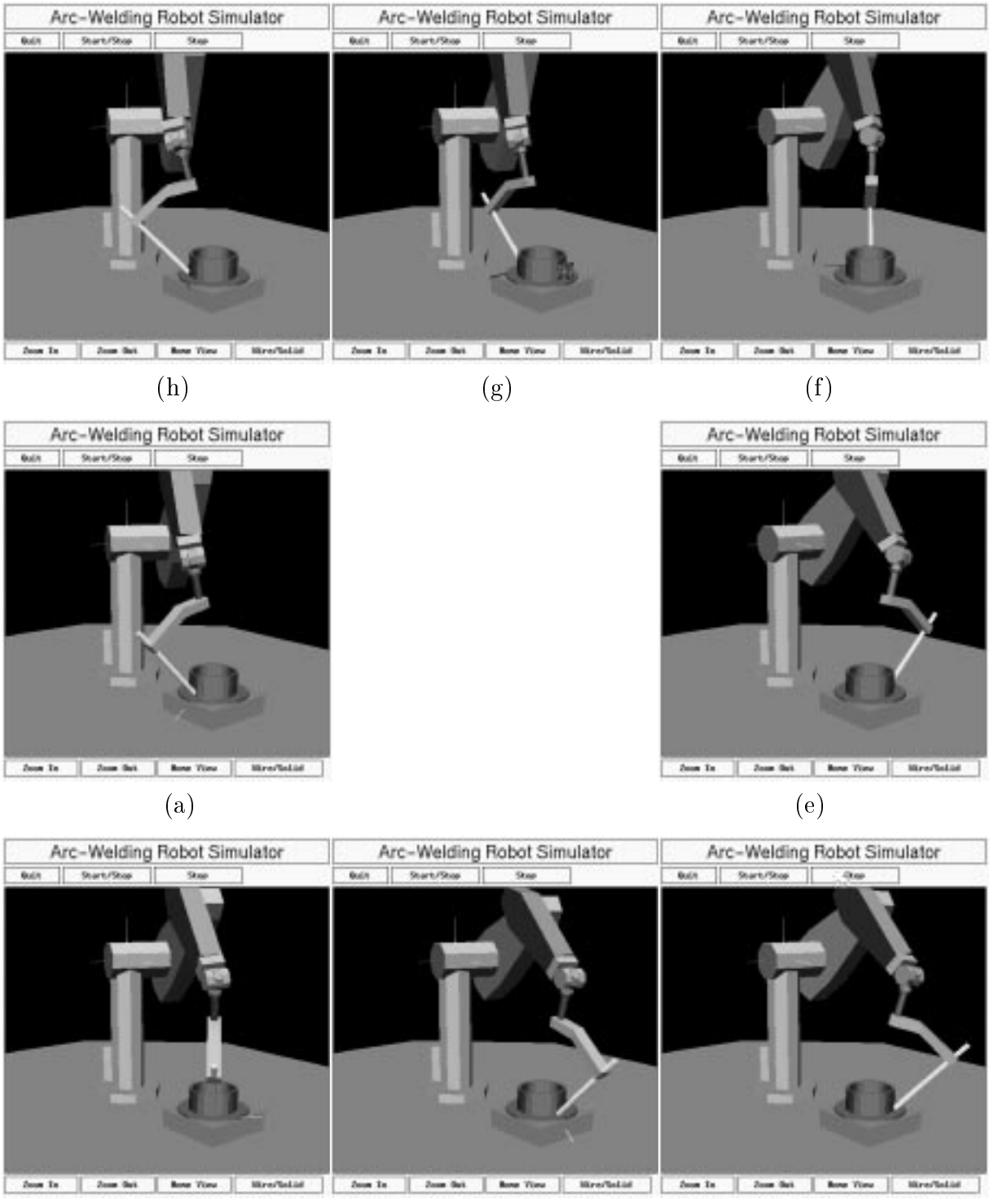

Figure 4: Arc-welding task without joint-limits avoidance strategy

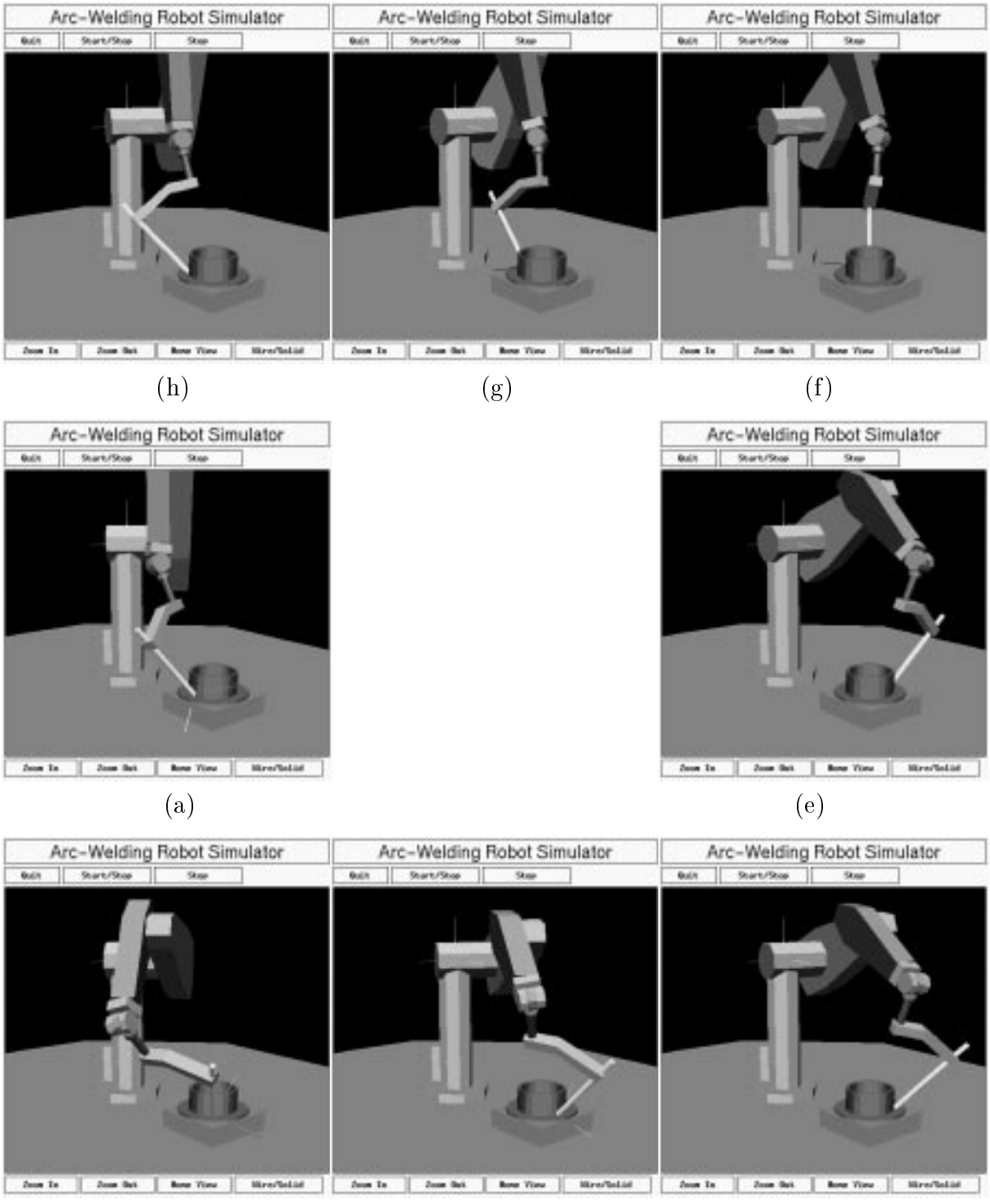

Figure 5: Arc-welding task with the mid-joint avoidance strategy

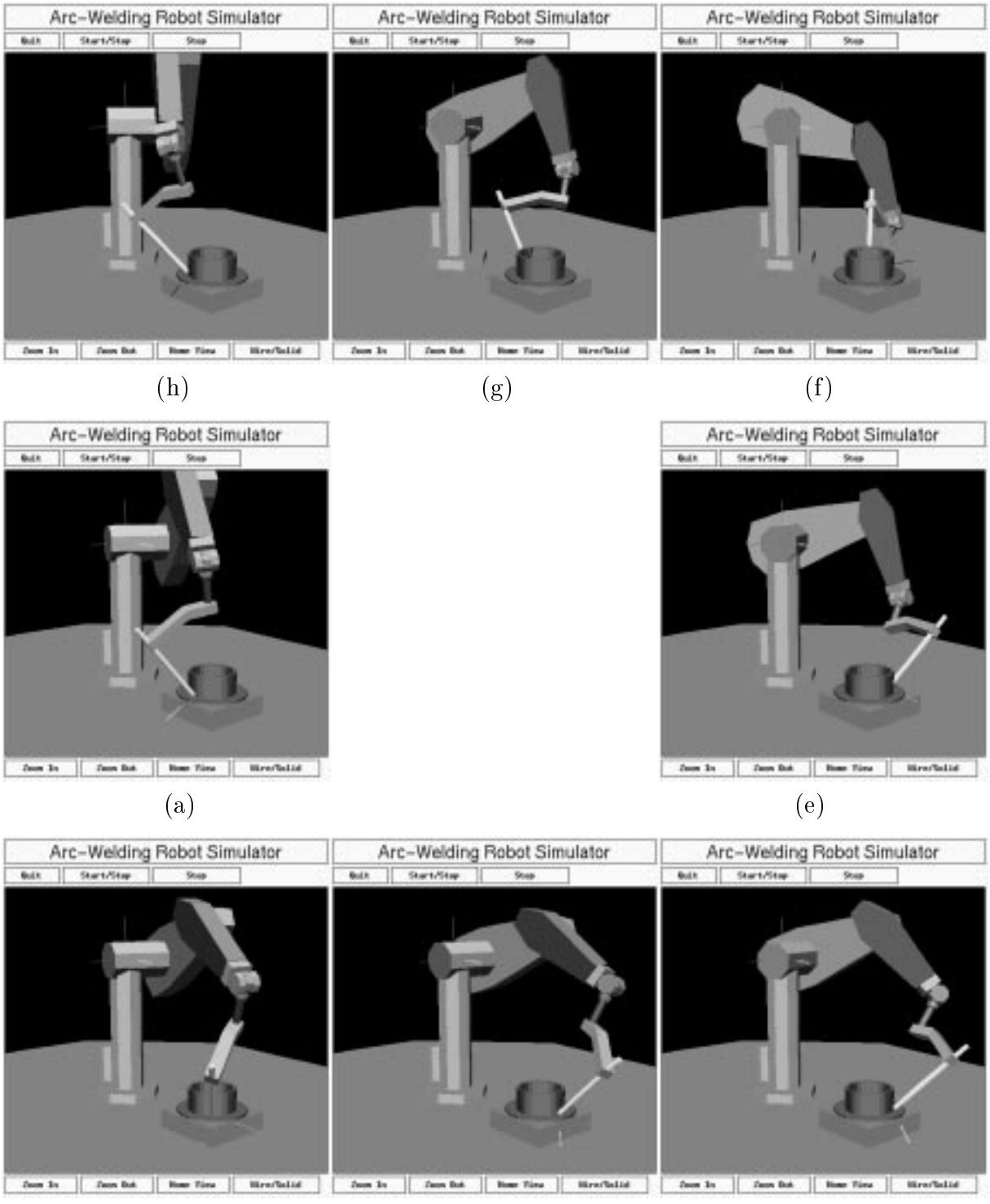

Figure 6: Arc-welding task with the mean-joint avoidance strategy